SIMULATION, Volume 96, Issue 4, April 2020, pp. 375-385
DOI: 10.1177/0037549719873969

A mimicking technique of back pressure in the hardware-in-the-loop simulation of a fuel control unit

Yuan Yuan[1], Zhiwen Zhao[2] and Tianhong Zhang[1*]

[1] Jiangsu Province Key Laboratory of Aerospace Power System, Nanjing University of Aeronautics And Astronautics, Nanjing, China

[2] Centre for Propulsion Engineering, School of Aerospace, Transport, and Manufacturing, Cranfield University, Central Bedfordshire, UK

Abstract

In the hardware-in-the-loop (HIL) simulation of the fuel control unit (FCU) for aero-engines, the back pressure has a great impact on the metered fuel, thus influencing the confidence of simulation. During the practical working process of an aero-engine, the back pressure of FCU is influenced by the combined effect of the pressure of combustion chamber, the resistance of spray nozzles, and the resistance of the distribution valve. There is a need to study the mimicking technique of FCU back pressure. This paper models the fuel system of an aero engine so as to reveal the impact of FCU back pressure on the metered fuel and come up with a scheme to calculate the equivalent FCU back pressure. After analyzing the requirements for mimicking the pressure, an automatic regulating facility is designed to adjust the FCU back pressure in real time. Finally, experiments are carried out to verify its performance. Results show that the mimicking technique of back pressure is well suited for application in HIL simulation. It is able to increase the confidence of simulation and provide guidance to the implementation of the mimicking of FCU back pressure.

Keywords: back pressure, HIL simulation, fuel control unit, aero-engine, mimicking technique

1. Introduction

Hardware-in-the-loop (HIL) simulation enables the operation and testing of actual components of a system along with virtual computer-based simulation models of the rest of the system in real time.[1,2] In this way, quality of testing is enhanced, thus shortening the design cycle and improving the reliability of the tested components.

Fuel control unit is a fuel-metering device that regulates the fuel flow to the engine in accordance with the pilot's demand, ambient environmental conditions, and other related factors. It is a crucial part of engine control system. Usage of HIL simulation for testing aero-engine FCU has been reported in several researches for different purposes. Montazeri-Gh et al.[3,4] have investigated the complex interaction between the FCU hardware and overall aircraft performance, while Karpenko and Sepehri[5] objectively tested novel fault tolerant control and diagnostics algorithms for fluid power actuators. Principles of the fuel control are presented by Tudosie,[6] among which the type with constant fuel differential pressure and

adjustable fuel window is most widely used. However, the performance of electro-hydraulic FCU can be influenced by changes in the characteristics of the operating environment and by changes in the system parameters.[3] As a result, whether the differential pressure across a fuel-metering valve could maintain constant remains a question. You et al.[7] investigated the influence of fluctuant inlet pressure on characteristics of FCU for a ramjet. Gaudet[8] has presented an approach for controlling fuel flow in which the differential pressure across a fuel-metering valve is regulated by simultaneously varying the pump displacement and a small amount of bypass flow.

In the practical fuel system of an aero-engine, fuel is injected into combustion chambers through the FCU, fuel distribution valve, and spray nozzles. So, the back pressure of FCU is equal to the sum of back pressure of spray nozzles, which is the outlet pressure of the engine compressor or the burner pressure, and pressure drop of fuel distribution valve as well as the spray nozzles. However, they both change with the operating state of the aero-engine. According to some researches,[9,10] fuel regulated by FCU is closely related to its back pressure. Regulating effects differ even in cases of same metering valve opening but different back pressure, which influences the confidence of simulation. So, it is necessary to adjust back pressure of FCU in real time. A common way to simulate the pressure is to use a throttle valve with either a fixed orifice or a manually adjusted orifice. It is readily apparent that its real-time performance cannot be guaranteed, which brings about new approaches. One of them is to simulate the atmospheric environment of the combustion chamber. This approach requires complicated devices and are of high cost. A much simpler way is to design an automatically adjusted valve that regulates the back pressure of the FCU according to the real-time engine state.

In this paper, mimicking technique of back pressure that is used in HIL simulations of FCUs for aero-engines is studied. In Section 2, mathematical model and AMESim model of the fuel system are established which reveal the working principle of each component. Then, the effect of FCU back pressure on metered fuel is investigated with the AMESim model in Section 3. Also, decisive factors of FCU back pressure and its calculation scheme are discussed in this part. Afterwards, requirements for simulating back pressure is put forward and an automatic regulating facility is finally designed in Section 4. Finally, in Section 5, experiments are conducted to verify the performance of the facility and its application in the HIL simulation.

2. Modelling of fuel system

In order to know how the FCU works, how its back pressure changes, and how it influences the metered fuel, each component of the fuel system should be analyzed. Taking a certain turbofan engine, for example, its fuel system includes a gear pump, FCU, fuel distribution valve and spray nozzle, while FCU includes a metering valve, a pressure drop valve, a fuel return valve, and a pressure rising valve, shown in Figure 1 and Figure 2. The gear pump is driven by high-pressure turbine after changing shaft speed by the gearbox. It generates flow with enough power to overcome pressure induced by the load at the pump outlet. The electro-hydraulic servo valve controlled by the electronic control unit (ECU) changes the pressure of control chamber of the metering valve, thus changing its displacement, which is then acquired by an LVDT displacement sensor and sent to the ECU for closed-loop control.[11] There is a

linear relationship between the opening area and displacement of the metering valve. The pressure drop valve senses the pressure at the inlet and outlet of the metering valve and adjusts the control fuel pressure of fuel return valve, so as to adjust the displacement of return valve, therefore adjusting the quantity of return fuel. If the pressure difference increases as the pump speed rises or the opening of the metering valve becomes smaller, the pressure drop valve feels the change of pressure difference and moves upwards, decreasing the control fuel pressure of the return valve. This leads to the upward movement of the return valve, resulting in the increase of return fuel and therefore the decrease of metered fuel. In consequence, the pressure difference is approximately held constant. Given this, fuel passing through the metering valve is only decided by its opening area, which means that ECU is able to control the fuel quantity by controlling the displacement of metering valve. The pressure increasing and the shut off valve act like “hydraulic resistance”, increasing the fuel pressure. Fuel metered by FCU is then distributed by the fuel distribution valve and sprayed into the combustion chambers.

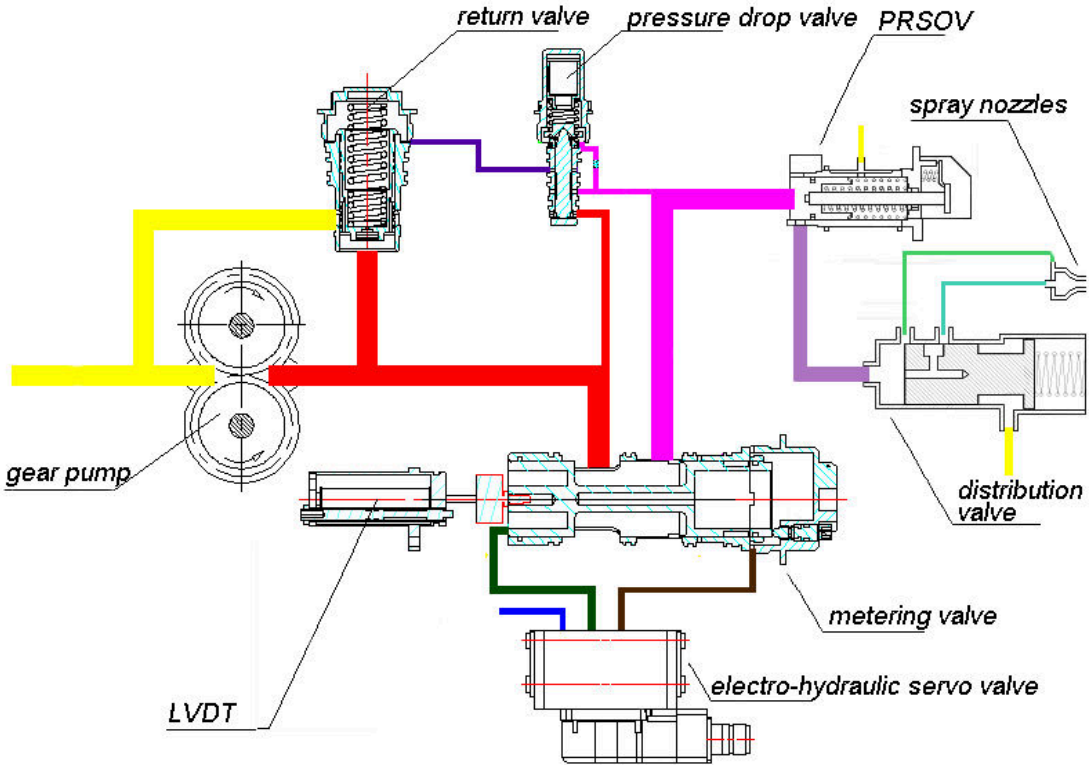

Figure 1. Components of fuel system.

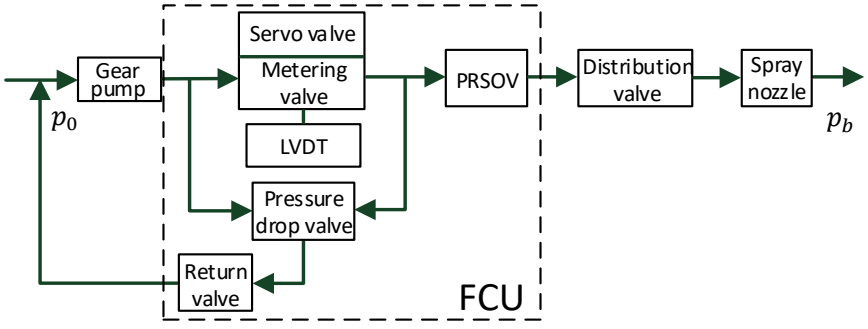

Figure 2. Schematic diagram of fuel system.

2.1 Mathematical model

2.1.1 Gear pump

The relationship between the fuel Q generated by the gear pump and its rotational speed n is given by the following equation:

$$Q = l \cdot n, \tag{1}$$

where l represents the fuel per rotation of the pump.

2.1.2 Fuel metering valve

The metering valve is the key component of the FCU, shown in Figure 1. It controls the fuel through the combustion chamber, called the metered fuel and denoted by Q_{fm}, which can be calculated with the following equation:

$$Q_{fm} = \mu_{fm} A_{fm} \sqrt{\frac{2(p_1 - p_2)}{\rho}}, \tag{2}$$

where μ_{fm} is the flow coefficient, A_{fm} is the opening of the metering valve, and ρ is the fuel density. p_1 and p_2 are the pressure at the inlet and outlet of metering valve respectively.

2.1.3 Pressure drop valve

The pressure drop valve maintains the difference of p_1 and p_2, whose structure is shown in Figure 3. p_1 and p_2 act on the right- and left-hand sides of the pressure drop valve, respectively. Force caused by the pressure difference balances the force of spring that is located in the left chamber of pressure drop valve when in a steady state, which yields the following:

$$(p_1 - p_2) A_{pd} = k_{pd} x_{pd}, \tag{3}$$

where A_{pd} is the spool area of pressure drop valve, k_{pd} is the spring stiffness, and x_{pd} is the spring compression.

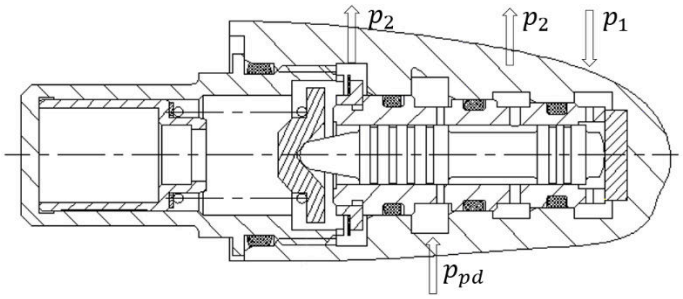

Figure 3. Structure of pressure drop valve.

2.1.4 Fuel return valve

The fuel return valve transmits the spare fuel to the inlet of the gear pump, whose structure is shown in the figure below. There is a center hole in the return valve, through which a portion of the inlet fuel of metering valve flows into the pressure drop valve and then combines with the outlet fuel of metering valve, forming a 'hydraulic potentiometer' whose working medium is the inlet fuel of metering valve.[12]

Fuel that flows through the center hole, denoted by Q_{fo}, can be computed as follows:

$$Q_{fo} = \mu_{fo} A_{fo} \sqrt{\frac{2\left(p_1 - p_{pd}\right)}{\rho}}, \tag{4}$$

where μ_{fo} is its flow coefficient, p_{pd} is its pressure, and A_{fo} is the area of the center hole. The fuel stated above joins the outlet fuel from metering valve. So, it can also be calculated as follows:

$$Q_{fo} = \mu_{fo} C_{pd} x_{pd} \sqrt{\frac{2\left(p_{pd} - p_2\right)}{\rho}}, \tag{5}$$

Where C_{pd} is the perimeter of the pressure drop valve.

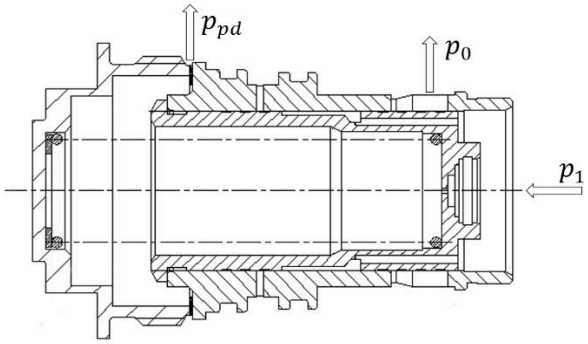

Figure 4. Structure of fuel return valve.

p_1 and p_{pd} are applied to the right- and left-hand side of the fuel return valve, respectively. The valve moves under these pressures so as to control its opening towards the inlet of the gear pump and therefore control the return fuel. When in a steady state, the force caused by the pressure difference balances the force of spring that is located in the left chamber of return valve, which yields the following:

$$\left(p_1 - p_{pd}\right) A_{fr} = k_{fr} x_{fr}, \tag{6}$$

where A_{fr} is the spool area of fuel return valve, k_{fr} is the spring stiffness, and x_{fr} is the spring compression. Fuel that returns to the inlet of the gear pump is given as follows:

$$Q_{fr} = \mu_{fr} C_{fr} x_{fr} \sqrt{\frac{2\left(p_1 - p_0\right)}{\rho}}, \tag{7}$$

where μ_{fr} is the flow coefficient, C_{fr} is the perimeter of valve, and p_0 is the low pressure.

Considering the fuel continuity, there is the following:

$$Q_{fm} + Q_{fr} + Q_{fo} = Q. \tag{8}$$

2.1.5 Pressure raising and shut off valve

The pressure raising and shut off valve, abbreviated as PRSOV, works as a 'hydraulic resistance', increasing the fuel pressure and shuts off the fuel sometimes. Figure 5 displays its structure. p_2 and p_{pr} act on the left- and right-hand side of PRSOV respectively. Force caused by the pressure difference balances the force of spring that is located in the chamber of PRSOV when in a steady state, which gives the following:

$$\left(p_2 - p_{pr}\right)A_{pr} = k_{pr}x_{pr}, \tag{9}$$

Where A_{pr} is the spool area of PRSOV, k_{pr} is the spring stiffness, and x_{pr} is the spring compression. Metered fuel flows through the PRSOV as follows:

$$Q_{fm} = \mu_{pr}C_{pr}x_{pr}\sqrt{\frac{2\left(p_2 - p_3\right)}{\rho}}, \tag{10}$$

where μ_{pr} is its flow coefficient, C_{pr} is the perimeter of valve, and p_3 is the outlet fuel pressure of PRSOV.

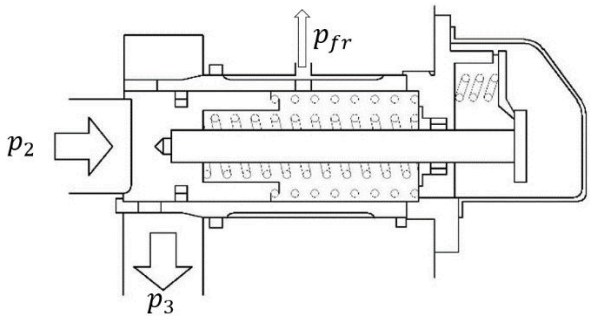

Figure 5. Structure of pressure raising and shut off valve.

2.1.6 Fuel distribution valve and spray nozzles

The fuel distribution valve distributes fuel into two kinds of combustion chambers, the first called the pre-burner and the second called main combustion chamber,[13] represented with $Q_{fd,s}$ and $Q_{fd,m}$,respectively. Then the spray nozzles atomize the fuel and spray it into the combustion chambers.[14] They can usually be treated as fixed orifices.

2.1.7 Steady-state model of fuel system

Based on equations stated above, the model that relates one variable to another can be derived. Take the inlet fuel pressure of the metering valve, p_1, and the pressure of combustion chamber, p_b, for example. Other models can be achieved in the same manner.

Substituting (3) into (5), then:

$$Q_{pd} = \frac{\mu_{pd}C_{pd}A_{pd}\left(p_1 - p_2\right)}{k_{pd}}\sqrt{\frac{2\left(p_{pd} - p_2\right)}{\rho}}. \tag{11}$$

Inserting (11) into (4) leads to the following:

$$K_1\sqrt{\left(p_1 - p_{pd}\right)} = K_2\left(p_1 - p_2\right)\sqrt{\left(p_{pd} - p_2\right)}, \tag{12}$$

where $K_1 = \mu_{fo}A_{fo}\sqrt{\frac{2}{\rho}}$, $K_2 = \frac{\mu_{pd}C_{pd}A_{pd}}{k_{pd}}\sqrt{\frac{2}{\rho}}$.

Substituting (6) into (7), then:

$$Q_{fr} = \frac{\mu_{fr} C_{fr} A_{fr} \left(p_1 - p_{pd} \right)}{k_{fr}} \sqrt{\frac{2\left(p_1 - p_0 \right)}{\rho}}. \tag{13}$$

Inserting (2) and (13) in (8) and considering that Q_{fo} is so samll compared to Q_{fm} and Q_{fr} that it can be neglected for simplicity leads to the following:

$$K_3 \sqrt{\left(p_1 - p_2 \right)} + K_4 \left(p_1 - p_{pd} \right) \sqrt{\left(p_1 - p_0 \right)} = Q, \tag{14}$$

where $K_3 = \mu_{fm} A_{fm} \sqrt{\frac{2}{\rho}}, K_4 = \frac{\mu_{fr} C_{fr} A_{fr}}{k_{fr}} \sqrt{\frac{2}{\rho}}$.

Combining (12) with (14) and eliminating p_{pd}, there is the following:

$$K_3 \sqrt{\left(p_1 - p_2 \right)} + K_4 \frac{K_1^{\,2} \left(p_1 - p_2 \right)^3}{K_1^{\,2} + K_2^{\,2} \left(p_1 - p_2 \right)^2} \sqrt{\left(p_1 - p_0 \right)} = Q. \tag{15}$$

This equation demonstrates the relationship between the inlet and outlet fuel pressure of metering valve, namely, p_1 and p_2, in steady state.

Given that fuel through the distribution valve and nozzle is continuous, the combined effect of the distribution valve and nozzle can be represented with an equivalent throttle facility, called “facility 1”. So, there is the following:

$$Q_{fm} = Q_{fd,m} + Q_{fd,s} = \mu_{eq1} A_{eq1} \sqrt{\frac{2\left(p_3 - p_b \right)}{\rho}}, \tag{16}$$

where μ_{eq1} is the flow coefficient of facility 1 and A_{eq1} is its area.

Similarly, fuel through the PRSOV and facility 1 is continuous. We can use another equivalent facility, called “facility 2”, to express their joint effect. Substituting (9) into (10), then combining with (16):

$$Q_{fm} = \mu_{eq2} A_{eq2} \sqrt{\frac{2\left(p_2 - p_b \right)}{\rho}}, \tag{17}$$

where μ_{eq2} is the flow coefficient of facility 2 and A_{eq2} is its area, and $\mu_{eq2} A_{eq2} = \frac{\left(\mu_{pr} C_{pr} x_{pr} \right)\left(\mu_{eq1} A_{eq1} \right)}{\sqrt{\left(\mu_{pr} C_{pr} x_{pr} \right)^2 + \left(\mu_{eq1} A_{eq1} \right)^2}}$.

Equation (17) and (2) present the same thing, which yields the following:

$$p_b = p_2 - K_5 \left(p_1 - p_2 \right), \tag{18}$$

where $K_5 = \left(\frac{\mu_{fm} C_{fm} x_{fm}}{\mu_{eq2} A_{eq2}} \right)^2$.

Solving (15) and (18), the relationship between p_1 and p_b in steady state is finally obtained:

$$K_3 \sqrt{\frac{p_1 - p_b}{1 + K_5}} + \frac{K_4 K_1^{\,2} \left(p_1 - p_b \right)^3}{K_1^{\,2} \left(1 + K_5 \right)^3 + K_2^{\,2} \left(1 + K_5 \right) \left(p_1 - p_b \right)^2} \sqrt{\left(p_1 - p_0 \right)} = Q. \tag{19}$$

In brief, it can be clearly seen from equation (15) that the pressure difference of the pressure drop valve will not always remain constant, resulting in the change of the metered fuel even in case of fixed A_{fm}. What is more, it is influenced by the nozzle back pressure in a complicated manner, since the model in (19) not only appears to be nonlinear but also has varying coefficients.

2.2 AMESim model

Since the mathematical model involves lots of variables and parameters, it is not likely to be comprehended intuitively and it is not convenient to get or display all variables such as force, displacement, flow resistance and so on. So, an AMESim model may facilitate the research. After analyses on the structure of each component, the model is established in Figure 6.[15,16]

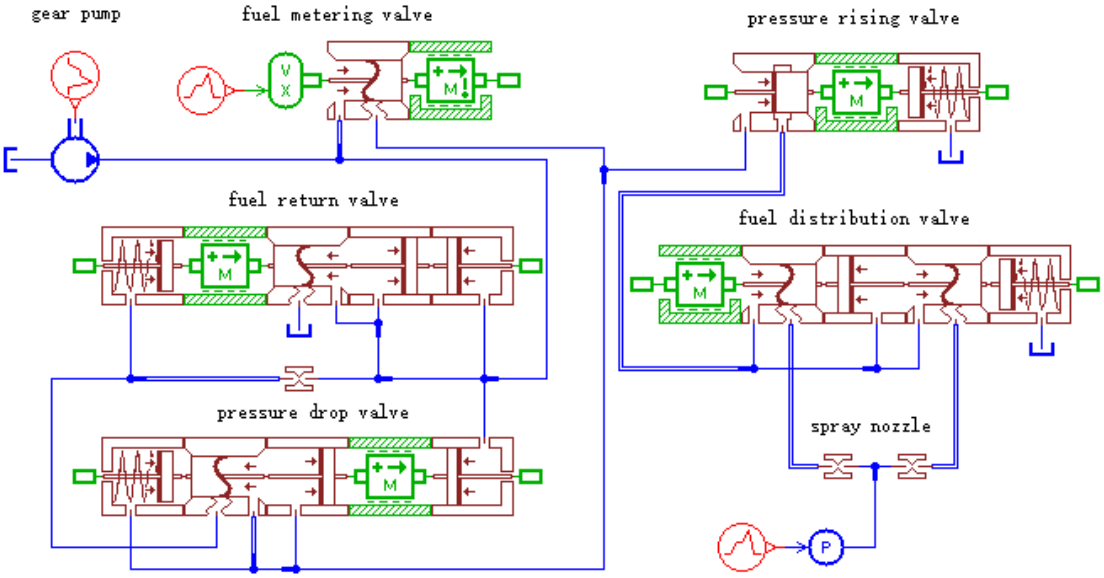

Figure 6. AMESim model fuel system.

3. Effect of FCU back pressure on metered fuel

3.1 Effect of nozzle back pressure on metered fuel

Firstly, the situation (denoted as situation 1) of the fixed opening of the metering valve (notified as A_{fm}) but different nozzle back pressure, namely p_b, are investigated, as shown in Figure 7. Increasing p_b from 6 bar to 10 bar at 6 s and from 10 bar to 14 bar at 13s, it can be seen from Figure 7(a) that both the inlet and outlet pressure of the metering valve, namely p_1 and p_2, increase accordingly. Meanwhile, metered fuel decreases from 16.27 to 16.03 and 15.97 L/min respectively, shown in Figure 7(b). This is the consequence of the movement of pressure drop valve. When p_b gets higher, p_2 becomes higher too, forcing the pressure drop valve to move rightward, thus loosening the spring, as depicted with a black line in Figure 7(c). As p_1 increases correspondingly, the spring force balances the pressure difference again, except for the reduction of spring compression, resulting in the decrease of $p_1 - p_2$, displayed with a red line. In conclusion, the metered fuel Q_{fm} reduces with the increase of nozzle back pressure p_b, which demonstrates the necessity of our research. In order to obtain a similar Q_{fm} in HIL

simulations as in actual situations, it is recommended that the precision tolerance of p_b be within 5%.

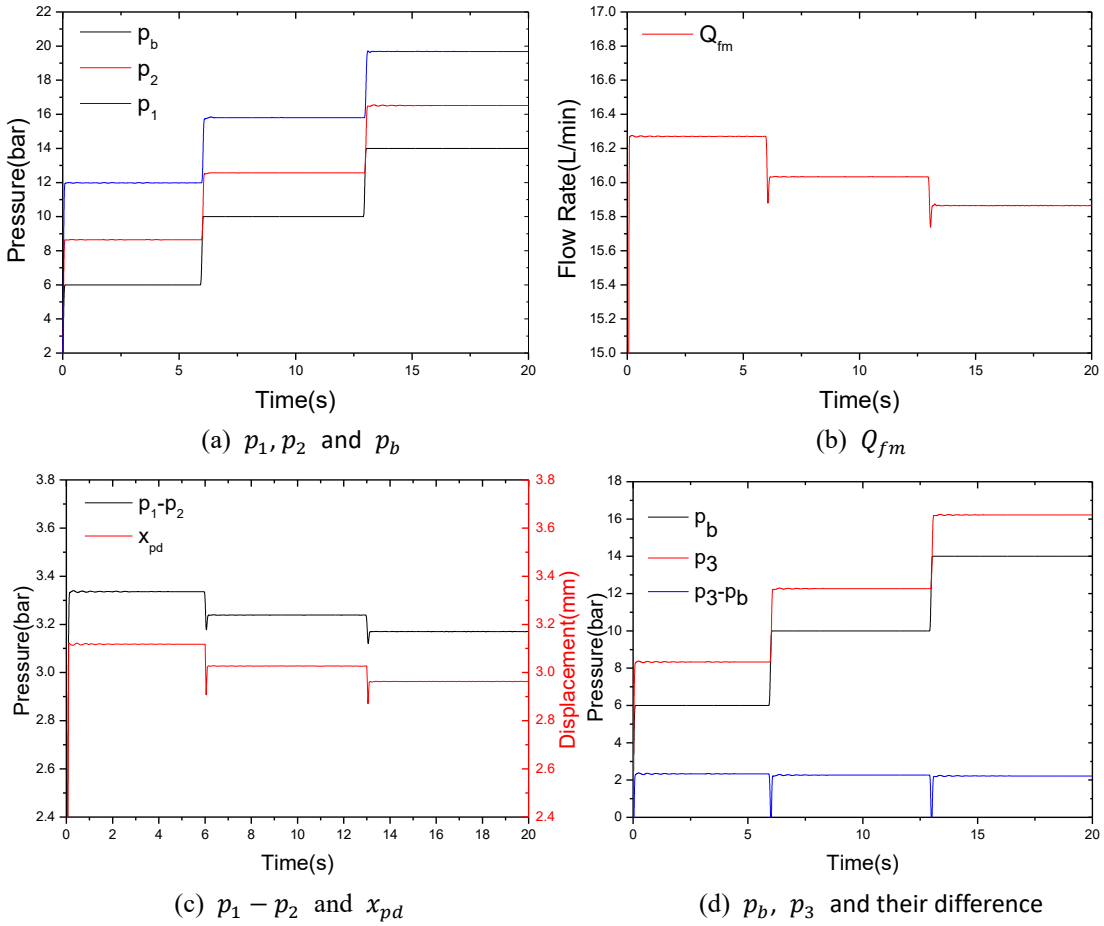

(a) p_1, p_2 and p_b (b) Q_{fm}

(c) $p_1 - p_2$ and x_{pd} (d) p_b, p_3 and their difference

Figure 7. Variables in situation 1.

3.2 Relation between FCU back pressure and nozzle back pressure

First considering the case in Section 3.1, the FCU back pressure p_3 grows with the nozzle back pressure p_b, shown as the red line and black line, respectively in Figure 7(d). However, their difference, depicted with the blue line, almost remains constant in this case. Then think about the situation (denoted as situation 2) of varying A_{fm} and fixed p_b, as we can see in **错误!未找到引用源。**. Increasing A_{fm} at 6 and 12.5s in a ramp and sinusoidal manner, respectively, Q_{fm} increases as expected. It can be seen that p_3 increases in the same manner simultaneously. In this regard, the difference between p_3 and p_b arises owing to the change of pressure drop in distribution valve and spray nozzles which is induced by the fuel change.

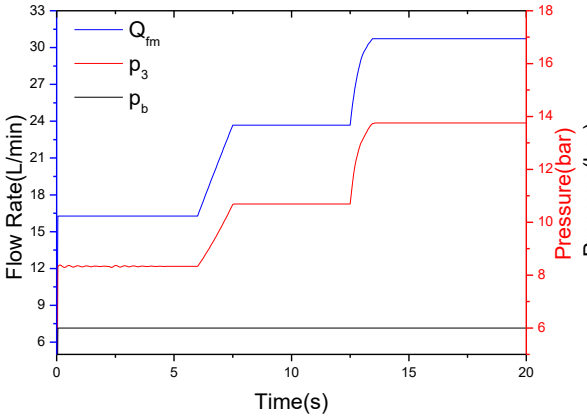

Figure 8. p_3 and Q_{fm} in situation 2.

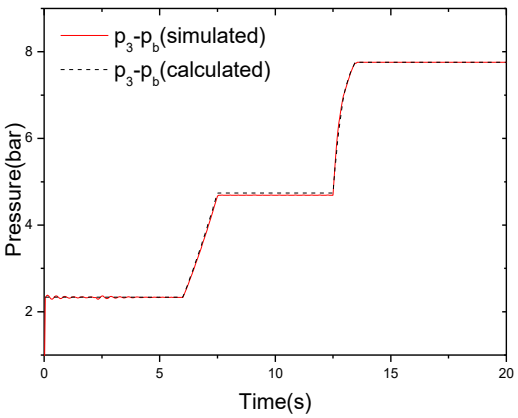

Figure 9. Calculated fuel control unit back pressure.

3.3 Calculation scheme for FCU back pressure

The results gained in Section 3.2 are on the premise of fixed A_{fm} or fixed p_b while actually both of them change in real time during operation of the engine.

From equation (16), the total pressure drop of fuel distribution valve and spray nozzles, denoted as Δp, can be obtained as follows:

$$\Delta p = p_3 - p_b = \frac{\rho Q_{fm}^{\ 2}}{2\left(\mu_{eq1} A_{eq1}\right)^2}. \tag{20}$$

It is readily apparent that Δp is proportional to the square of Q_{fm} and inversely proportional to the square of $\mu_{eq1}A_{eq1}$. Suppose there is a steady point D, and let:

$$\alpha = \frac{\Delta p_{,D}}{Q_{fm,D}^{\ 2}}, \tag{21}$$

where, the subscript D denotes the specific value of Δp and Q_{fm} around point D. Then, (20) can be approximated as follows:

$$\Delta p = \alpha \cdot \beta \cdot Q_{fm}^{\ 2}, \tag{22}$$

where β is termed as compensating factor, which serves to compensate the error introduced by $\mu_{eq1}A_{eq1}$. As Q_{fm} increases, the distribution valve opens up and x_{fd} is therefore enlarged, which leads to the increase of $\mu_{eq1}A_{eq1}$. So β ought to be reduced with the increase of Q_{fm}. β can be obtained from simulations, experiments or the approximate formula as follows:

$$\beta = \left(\frac{Q_{fm,D}}{Q_{fm}}\right)^m, \tag{23}$$

where, m can be selected or adjusted based on actual situations, usually ranging from 1/12 to 1/2. β is equal to 1 at steady point D.

Consider the situation in Section 3.2. Selecting a steady point where $Q_{fm,D}$ is 30.728 L/min, $\Delta p_{,D}$ is 7.74 bar, then α is equal to 8.216×10^{-3}. Selecting m=1/8, then Δp can be calculated with (22), as is depicted with the black and dashed line in Figure 9, while the red line is the simulated value of Δp in

Section 3.2. The difference is so small that we can use Equation (22) to compute Δp. Hence, the FCU back pressure p_3 is gained:

$$p_3 = \alpha \cdot \beta \cdot Q_{fm}{}^2 + p_b. \tag{24}$$

4. Mimicking scheme for FCU back pressure

In this section, we talk about how to design a facility that regulates p_3 automatically while satisfying the requirements for HIL simulation. So, firstly requirements for simulating p_3 are discussed and then the regulating facility is schemed out.

4.1 Requirements for the mimicking of FCU back pressure

Starting with requirements for the settling time of p_3, we should first investigate the operation process of the engine, that is, from idling state(speed) to maximum state(speed). A schematic demonstrating the closed-loop control of the engine speed is shown in Figure 10. It consists of two loops, inner loop called the control loop of metered fuel and an outer loop called the control loop of rotational speed. The principle of inner loop has been described in the foreword of Section 2. In the outer loop, the engine speed is collected and sent to ECU for the comparison with the instructed rotational speed, thus figuring out the instructed position of the metering valve and adjusting metered fuel through inner control loop. Meanwhile, the rotational speed decides the fuel generated by the gear pump and the outlet pressure of compressor influences the fuel metered by the FCU. It is believed that the settling time of p_3 corresponds to that of rotational speed or metered fuel. In general, the speed settling time of an aero-engine from idling to maximum is around 5-6 s.[13,17] Therefore, the regulating facility should at least be able to follow the settling time of p_3, that is, 5 s from the idling to the maximum. Furthermore, the bandwidth of regulating facility should be wider than that of the fuel control loop, which is generally a value of 2~3Hz.

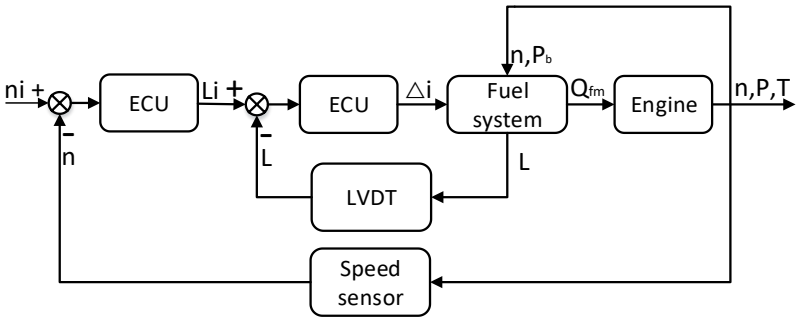

Figure 10. Schematic diagram of engine speed control loop. ECU: electronic control unit.

So, integrated with Section 3, for the requirements for simulating p_3, it is put forward that the precision tolerance of p_3 should be within 5%, the settling time of p_3 ought to be less than 5 s from idling to maximum, and the bandwidth of the regulating facility should be over 3Hz.

4.2 Design of the automatic regulating facility

Coming next is the design of automatic regulating facility based on the requirements described in

Section 4.1. The working principle of the facility is shown in Figure 11. It is also comprised of two control loops. A throttle valve is installed at the outlet of FCU, the opening of which can be adjusted by the valve rod. A motor is attached to the valve, turning the valve rod. The displacement of the rod, namely the position of the valve, is acquired by a permanent linear contactless displacement (PLCD) sensor, which is installed normal to the rod sent back to the controller. Fuel flows through the valve and thus generates pressure. The pressure is then collected by a pressure sensor and sent to the controller. Together with the instructed pressure calculated with Equation (24), an instructed position of the valve is figured out. Comparing it with the real position from the PLCD sensor, the deviation generates pulse signals that adjusts the valve rod so as to changes the valve opening, thereby regulating the fuel pressure. Finally, the automatic regulating facility comes out, as shown in Figure 12.

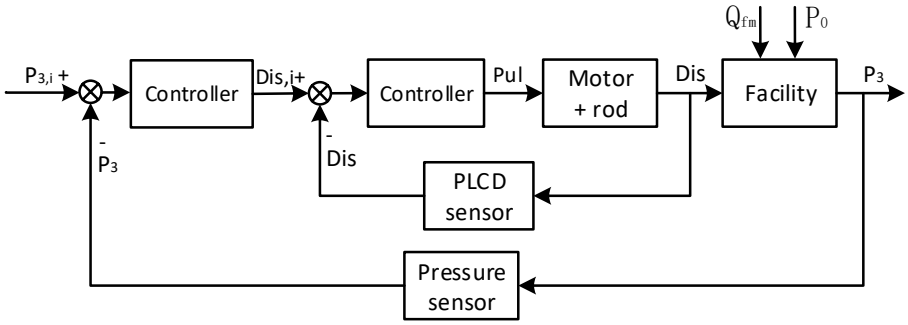

Figure 11. Principles of the automatic regulating facility. PLCD:

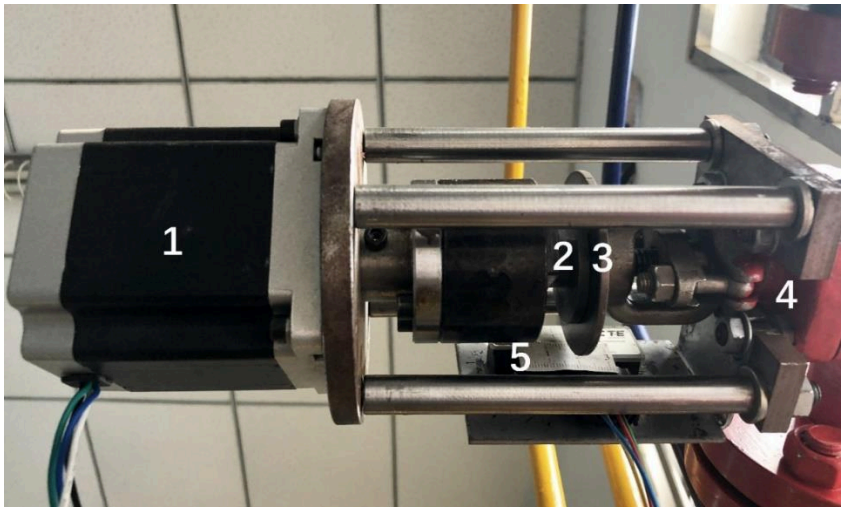

Figure 12. The automatic regulating facility. 1: motor; 2: rod; 3: magnetic ring; 4: valve; 5: permanent linear contactless displacement.

5. HIL simulation based on FCU back pressure

Now that the automatic regulating facility of the FCU back pressure has been designed, it is time to carry out experiments for the purpose of validating its regulating ability and its application in HIL simulations. The test platform is as shown in Figure 13.

Figure 13. HIL simulation test platform. 1: fuel tank; 2: booster pump; 3: fuel control unit; 4: automatic regulating facility; 5: controller; 6: pressure transducer; 7:flow meter.

5.1 Validation of the regulating ability of FCU back pressure

Keeping the metered valve at the maximum opening and adjusting the instructed p_3, the experimental result (denoted as situation 3) is exhibited in Figure 14. The black line in Figure 14(a) indicates the instructed p_3 and the red line represents the real p_3. It is viewed that the real p_3 is able to keep up with the change of instructed p_3. From the partially enlarged view, it can be seen that when the instructed p_3 is increased from 26.8 to 34.1 bar at 13.7 s, the real p_3 matches well with it in about 1 s, with a delay of 300 ms and no overshoot. The error of steady-state values is within 0.4 bar. As is seen in the experiments, the steady-state error is within 0.5 bar throughout the whole regulating process. So, the facility is able to satisfy the requirements of accuracy. Given that the regulation range of p_3 is from 10 to 50 bar, a variation of 7.3 bar is a very large step and it only takes 1 s to settle down. So, the automatic regulating facility can satisfy the requirement for real-time simulations.

In addition, the black line in Figure 14(b) shows the change of Q_{fm} as a result of the change of p_3, shown by the red line. The result proves the conclusion in Section 3, that Q_{fm} reduces with the increase of p_3.

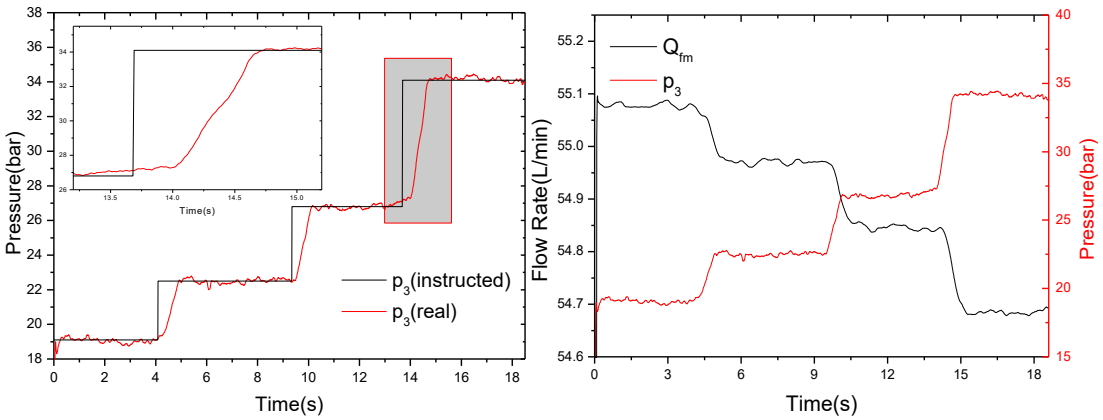

(a) Instructed l p_3 and real p_3 (b) Q_{fm}

Figure 14. Variables in situation 3.

5.2 HIL simulation of an FCU based on the mimicking technique of back pressure

In order to apply the mimicking technique to practice and verify its performance, a HIL simulation (denoted as situation 4) is carried out. Adjusting the instructed rotational speed from idling to maximum step by step, with the blue and dashed line in Figure 15(a), the real engine speed shown with the red line varies correspondingly and settles down in complete agreement. Beyond doubt this is a result of the change of metered fuel, displayed with a black line. Q_{fm} brings about the change of operation state, including p_3, which is the instructed p_3, shown with a black line in Figure 15(b). Then the automatic regulating facility reacts, leading to the change of real p_3, shown with a red line. We can see that the real p_3 follows the instruction as desired. In turn, the back pressure influences the metered fuel. It can be seen from the enlarged view in Figure 15(a) that when instructed speed increases from 86.6% to 92.8% at 40.15 s, the real speed follows in 0.8 s. The Q_{fm} also settles down in 0.9 s. From the enlarged view Figure 15(b), the instructed p_3 increases from 23.9 to 29.1 bar in 0.5 s and only jitters on a very small scale. The real p_3 responds with a delay of about 150 ms and no remarkable overshoot. The setting time is about 0.8 s with a steady state error of nearly 0.1 bar. Throughout this simulation, the settling time for a large step change of p_3 is no more than 1 s and its steady error is within 2%

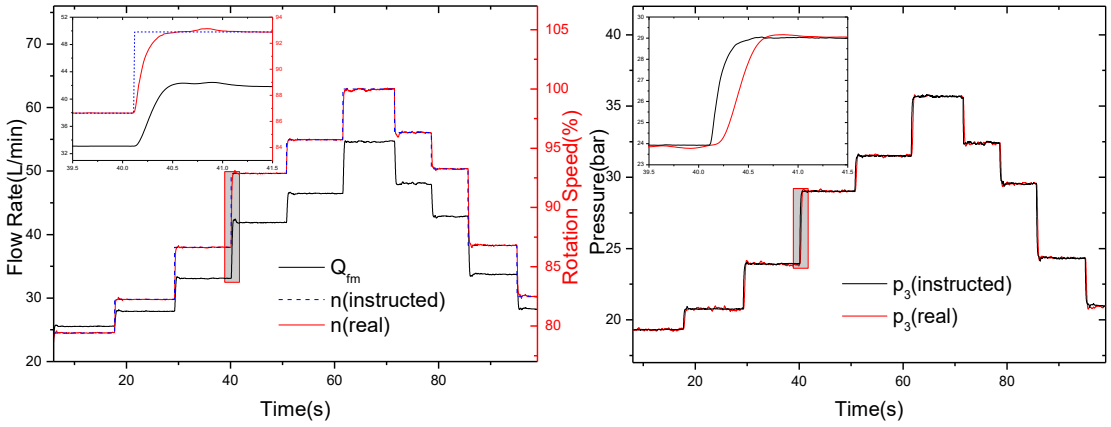

(a) Instructed *n*, real *n* and Q_{fm} (b) Instructed and real p_3

Figure 15. Variables in situation 4

6. Conclusion

This paper studies the mimicking technique of back pressure, which is used in HIL simulations of FCUs for aero-engines. First, it establishes models of the fuel system, which reveals the working principle of each component. Then, the effect of FCU back pressure on metered fuel is investigated with the AMESim model, and it is found that the metered fuel reduces with the increase of back pressure. Afterwards, the determinants of FCU back pressure are discussed, thus coming up with the calculation scheme for its application in HIL simulations. After that, the mimicking scheme for FCU back pressure is hammered out. The requirements for simulating the pressure are put forward before we design an automatic regulating facility. Finally, experiments are conducted to verify the performance of the facility and its application in the HIL simulation. Results show that throughout this simulation, the settling time

of FCU back pressure controlled by the automatic regulating facility for a large step change is no more than 1 s and its steady error is within 2%, which proves its application in the HIL simulation and increases the confidence thereof.

Acknowledgments

This work was supported by Postgraduate Research & Practice Innovation Program of Jiangsu Province (KYCX19_0186).

ORCID iD

Yuan Yuan_ https://orcid.org/0000-0002-6489-4563

Zhiwen Zhao_ https://orcid.org/0000-0002-4836-030X

References

1. Fathy HK. Review of hardware-in-the-loop simulation and its prospect in the automotive area. In: Schum K and Sisti AF (eds) Society of Photo-optical Instrumentation Engineers, proceedings of SPIE 6228, Orlando, FL, May 2006, pp. 1–20. Washington, DC: SPIE.

2. Bradley TH, Moffitt BA, Mavris DN, et al. Hardware-in-theloop testing of a fuel cell aircraft powerplant. J Propulsion Power 2012; 25: 1336-1344.

3. Montazeri-Gh M, Nasiri M, Rajabi M, et al. Actuator-based hardware-in-the-loop testing of a jet engine fuel control unit in flight conditions. Simulat Model Pract Theor 2012; 21: 65-77.

4. Montazeri-Gh M and Nasiri M. Hardware-in-the-loop simulation for testing of electro-hydraulic fuel control unit in a jet engine application. Simulation 2013; 89: 225-233.

5. Karpenko M and Sepehri N. Hardware-in-the-loop simulator for research on fault tolerant control of electrohydraulic actuators in a flight control application. Mechatronics 2009; 19: 1067-1077.

6. Tudosie AN. Aircraft gas-turbine engine's control based on the fuel injection control. In: Mulder M (ed.) Aeronautics and astronautics. Rijeka: InTech, 2011.

7. You Y, Zhao S, Wu B, et al. A simulation on dynamic characteristics of ramjet fuel regulator based on AMESim. J Rocket Propulsion 2010; 36(4): 12–15.

8. Gaudet TJ. Hydromechanical control for a variable delivery, positive displacement fuel pump. In: ASME 1999 international gas turbine and aeroengine congress and exhibition, 1999, Indianapolis, IN, 7–10 June 1999, V004T04A005. New York: American Society of Mechanical Engineers

9. Suo J and He L. Theoretical study on the spray characteristics of plain jet atomization under high back pressure. In: 43rd AIAA/ASME/SAE/ASEE Joint Propulsion Conference & Exhibit, Cincinnati, OH, 8–11 July 2007, pp. 5689–5693. Reston, VA: AIAA.

10. Ziraksaz MH. An experimental study on fuel atomization in pressurized injectors. In: AIAA/ASME/SAE/ASEE joint propulsion conference & exhibit, Denver, CO, 2–5 August 2009, pp. 5405–5413. Reston, VA: AIAA.

11. Georgantas A, Krepec T and Cheng R. Design optimization of an electronic fuel control unit featuring two digital actuators. In: 27th joint propulsion conference, Sacramento, CA, 24-26 June 1991, pp. 2003–2012.
12. Yao H and Zhang TH. Control system design technology for aero-engine. Beijing: Science Press, 2017.
13. Bumb A and Hawk C W. History of staged combustion cycle development. In: 29th Joint Propulsion Conference and Exhibit, Monterey, CA, 28 June – 30 June 1993, pp. 3234–3251. Reston, VA: ARC.
14. Shang H, Kim Y, Chen C, et al. Studies on fuel spray characteristics in high-pressure environment, Nashville, TN, 6–8 July 1992, pp. 3234–3251. Reston, VA: AIAA.
15. Li HC, Zhang HA, Han XB, et al. Research on the real-time model of aero-engine actuator. Appl Mech Mater 2014; 568- 570: 1036-1040.
16. Antonelli M, Baccioli A, Francesconi M, et al. Small scale ORC plant modeling with the AMESim simulation tool: analysis of working fluid and thermodynamic cycle parameters influence. Energ Proced 2015; 81: 440-449.
17. Jaw LC and Mattingly JD. Aircraft Engine Controls Design, System Analysis and Health Monitoring. Reston, VA: American Institute of Aeronautics and Astronautics. Inc., 2009.

A mimicking technique of back pressure in the hardware-in-the-loop simulation of a fuel control unit

Yuan, Yuan

2019-09-17

Yuan Y, Zhao Z, Zhang T. (2020) A mimicking technique of back pressure in the hardware-in-the-loop simulation of a fuel control unit. SIMULATION, Volume 96, Issue 4, April 2020, pp. 375-385

https://doi.org/10.1177/0037549719873969